LOW-TEMPERATURE EXTRA ORDERING EFFECTS IN SYMMETRIC BLOCK COPOLYMERS FROM LATTICE MONTE CARLO SIMULATION

S. WOLOSZCZUK[1], M. BANASZAK[1]*, S. JURGA[1] AND M. RADOSZ[2]

*Institute of Physics, A. Mickiewicz University
Umultowska 85, 61-614 Poznań, Poland*

*Department of Chemical and Petroleum Engineering, University of Wyoming Laramie
IVY 82071-3295, USA*

Abstract: Lattice computer simulations of block copolymer melts are reported. Low-temperature lamellar ordering conjecture is presented and its justification is provided. In addition to reviewing the previous data we present a new evidence for the extra ordering effects by recording the mean squared rotational angles as a function of the reduced temperature.

1. INTRODUCTION

Block copolymers can self-assemble into a variety of ordered microstructures [1], which opens up numerous practical applications, for example, in nanotechnology. A single block is a sequence of covalently bonded monomers of the same chemical type, and individual blocks differ in the monomer types. Diblock copolymers are made up of two chemically distinct blocks connected in A-B sequence. In case of triblock copolymers we have two possibilities: two chemically distinct blocks connected in A-B-A sequence or three chemically distinct blocks connected in A-B-C sequence. Such block copolymers can self-assemble into ordered microstructures, such as *bcc* spheres, spatially ordered layers, or hexagonally packed cylinders. Apart from these classical microstructures there are others, such as ordered bicontinuous double diamond structures, gyroid bicontinous structures and hexagonally packed layers, of which only the gyroid structure is known to be stable for pure diblock copolymers. Those microstuctures can be obtained by cooling the copolymer melt from a high-temperature disordered state to a low-temperature ordered state, which can be characterized by an order-disorder transition (ODT) temperature, T_{ODT}. This temperature marks the onset of long-range order. However, the phase separation on a macroscopic scale is impossible due to connections between chemically incompatible blocks. The phase behavior of symmetric triblock copolymers, *i.e.,* two external blocks of the chain are of the same length, is similar to that of the corresponding diblock copolymers [2, 3]. This is easy to understand when one

---

* Corresponding author: e-mail: mbanasz@amu.edu.pl

realizes that cutting the symmetric triblock in a middle produces two diblocks. The entropy gained from doing this is relatively small.

The mechanical properties of diblock copolymers and the corresponding A-B-A triblock copolymers differ significantly. This is because the possible arrangements of the triblock chains are different from those of diblock chains. In particular, the triblock chains can form looped and bridged configurations [4-6]. When the triblock chain ends belong to the same interface, it forms a loop, but when the chain terminal blocks are located in two different interfaces separated by a microdomain containing its middle block, we have a bridge. One can control the loops to bridges ratio to achieve a desired degree of catenation between the neighboring layers. This is not applicable to diblocks.

Recently we showed [5, 6], by a lattice Monte Carlo simulation, that at very low temperatures (well below T_{ODT}) the conventional slow cooling scheme yields results which largely do not agree with the experimental data and theory. Such thermal treatment lead to lamellar spacing and orientation trappings as the temperature was lowered. Therefore we used an alternative method, referred to as quenching, where the system was instantaneously cooled down to the required temperature from an a thermal state. The results, obtained from the simulations performed by the quenching method, were in a significantly better agreement with theory and experiment. Moreover, we recorded extra low-temperature effects which were not present in the slow cooling scheme, such as an additional peak in the specific heat. These effects were accompanied by an interfacial ordering from a strongly segregated, but still considerably diffused lamellar phase, to a more strongly segregated phase with a smooth and sharp interface. It was not clear, however, whether these effects were to be solely attributed to the underlying lattice or whether they were there regardless of the lattice.

In order to verify this low-temperature ordering conjecture, we performed a series of simulations with box sizes which were varied systematically. Moreover, we focused our attention on the symmetric diblock copolymer melts [7], rather than a triblock melt studied previously. Similarly as for triblocks, we performed quenches and the extra low-temperature effects were also recorded. This suggests that the appearance of recorded effects does not depend on the box size nor on the copolymer microarchitecture.

In this paper we briefly review our work on low-temperature effects [5-7] in symmetric block-copolymer melts and provide an additional evidence for those effects by presenting results for the temperature dependence of the rotational diffusion.

2. MODEL AND SIMULATION METHOD

The simulations were performed using the Cooperative Motion Algorithm (CMA) [8], developed by Pakula and co-workers as presented in Ref. [5]. CMA is a model of lattice liquid which, in contrast to lattice gas, doesn't require any vacancies to perform the rearrangements. The algorithm is based on the Face Centered Cubic (FCC) lattice with coordination number z

= 12 and the bond equal to $\sqrt{2}a$, where a is the FCC lattice constant. Bonds are not allowed to be broken or stretched, and the usual periodic boundary conditions are satisfied. For the symmetric 7-16-7 triblock copolymer melt we use 30 x 30 x 30 and 60 x 30 x 30 simulation boxes. For the symmetric 8-8 diblock copolymer melt, on the other hand, we use the following four simulation boxes: $30 \times 32 \times 30$, $40 \times 32 \times 30$, $50 \times 32 \times 30$, and $60 \times 32 \times 30$. The number of chains can be calculated as n_a/N, where n_a is the number of lattice sites, and N is the number of chain segments; $N = 16$ for diblocks and $N = 30$ for triblocks. For example, the 30×30 x 30 lattice is filled with $n_a/N = 450$ triblock chains of length $N = 30$, whereas the 30 x 32 x 30 lattice is occupied with $n_a/N = 900$ diblock chains of length $N = 16$. The lattice sites are completely filled with monomers and there are no vacancies. The interaction energy between monomers is given by ε_{ij}, where $\varepsilon_{AA} = \varepsilon_{BB} = 0$, and $\varepsilon_{AB} = \varepsilon$. The interaction is limited to the nearest neighbors (=12), and the interaction parameter, ε is related to the Flory χ parameter by the following equation:

$$\chi = \frac{(z-2)}{k_B T}. \tag{1}$$

This parameter serves also as an energy unit to define the reduced energy and the reduced temperature as

$$E^* = E/\varepsilon, \tag{2}$$

$$T^* = k_B T / \varepsilon. \tag{3}$$

3. RESULTS AND DISCUSSION

We start the simulation by equilibrating the system in an athermal state, where $\varepsilon/(k_B T)$ is zero. The system is thermally equilibrated when the polymer chains assume their statistical conformations and random orientations and become uniformly distributed within the simulation box.

In this way we prepare three statistically independent configurations for the triblocks and ten configurations for the diblocks. From each of those configurations the system is quenched to the required temperature with equilibration time set to at least 3×10^6 MC steps. An attempt to move a single monomer is assumed to define a single MC step. Usually the first 1.5×10^6 MC steps are to equilibrate the system, and the next to sample the data. At selected temperatures, however, we perform up to 200×10^6 MC steps in order to monitor the relevant thermodynamic, structural and dynamic properties.

First we turn our attention to the triblocks. In Fig. 1 we report the total interaction energy per lattice site, E^*/n_a, the specific heat calculated as

$$C_V = \frac{\left\langle \left(E^* - \left\langle E^* \right\rangle\right)^2 \right\rangle}{n_c T^{*2}}, \tag{4}$$

where $n_c = n_a/N$ is the number of chains in simulation box, and the variations of the equilibrium end-to-end distance of the diblock chain, R^2, as a function of the reduced temperature. The reduced temperature is divided by the degree of polymerization, N, since according to Leibler's RPA theory for pure diblock melts [9] the ODT temperature T^*_{ODT} scales linearly with chain length, N. The energy per lattice site decreases as the temperature is decreased, with the fastest change close to $T^*/N = 0.28$. Taking into account all results for the 7-16-7 triblocks, we identify T^*/N 0.28 as the ODT temperature.
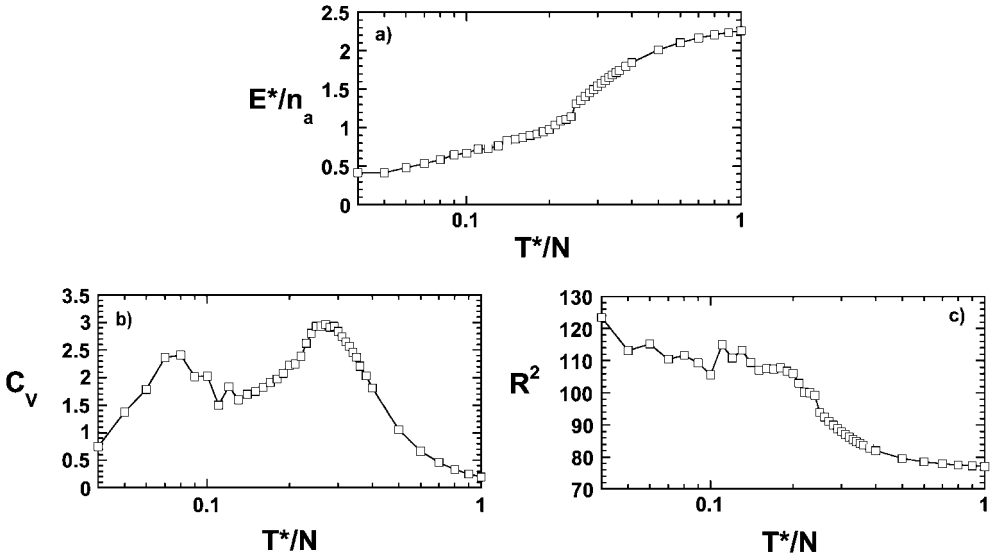
Fig. 1. Simulation results for the 7-16-7 triblock copolymers: (a) energy per lattice site, E_*/n_a; (b) specific heat, C_V; (c) squared end-to-end distance, R^2

Next we report two C_v maxima in Fig. 1b: the first one close to $T^*/N = 0.28$ and the second one at $T^*/N = 0.08$. The first one is associated with order-disorder transition, whereas the possible meaning of the low-temperature one, as somehow corresponding to an additional interfacial ordering, is discussed below with the presentation of the other data. Figure 1c presents the squared end-to-end distance, R^2, as a function of reduced temperature. At high temperatures R^2 of the triblock is quite close to the Gaussian value, $(N - 1)a^2 = 58$, and increases significantly indicating chain extension as the temperature is decreased towards T_{ODT}. At relatively low-temperatures (those corresponding to the second C_v peak) one can notice bigger R^2 variations and also one more rapid chain extension. We have to stress here, that these low-temperature peak is noticeable only in the quenching experiments, where the

system enjoys effectively more freedom in probing the phase space and choosing the lamellar spacing.

In order to explore more quantitatively the above low-temperature effects, we introduce the interfacial parameter, Λ. This parameter describes the degree of smoothness of interfaces between two different neighboring domains, and decreases as the interfaces become more smooth. When all the junction points fit into a perfect two-dimensional plane, the parameter Λ is zero. At very low temperatures we calculate Λ for a given lamellar interface as

$$\Lambda = \frac{\sum_{i=1}^{M}\left(\overline{r}-r_i\right)^2}{M}, \tag{5}$$

where M is the number of junction points within a given interface, $\overline{r}$ is $\left(\sum_{i=1}^{M} r_i\right)\!\Big/ M$, and r_i are calculated as

$$r_i = \vec{r_i} \cdot \vec{n} \tag{6}$$

with $\vec{r_i}$ denoting the position of i-th junction point in the simulation box ($i = 1, 2, ..., M$). The last term in Eq. (6) is the normalized vector, $\vec{n}$, perpendicular to layers, which can be written as:

$$\vec{n} = \frac{\left(x,y,z\right)}{\sqrt{x^2+y^2+z^2}}. \tag{7}$$

We determine that vector by calculating the monomer concentration profiles in a large number of directions [x, y, z], where $x, y, z = -m, -m + 1, ..., m,$ and m is an integer. In our case $m = 16$. The direction in which the variations of the squared difference between concentration profiles, $(\varphi_A - \varphi_B)^2$, reach their maximum, is the desired direction perpendicular to layers. The parameter Λ is averaged over all interfaces in the simulation box with the weights proportional to the number of junction points within a given interface. In the case of 7-16-7 triblocks the junction points are calculated as lying between the 7th and 8th segment, and also between the 23rd and 24th segment.
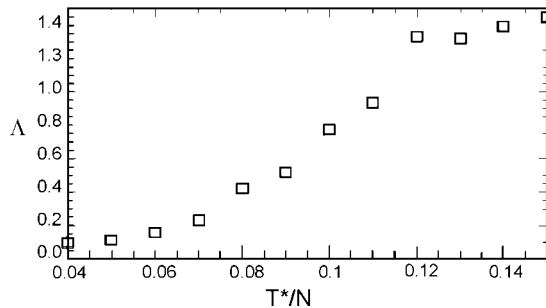
Fig. 2. Interfacial parameter, Λ as a function of T^*/N for 7-16-7 microarchitecture

In Figure 2 we report the parameter Λ as a function of reduced temperature in the vicinity of the low-temperature C_V peak. We can clearly see that above the temperature $T^*/N = 0.12$ the parameter Λ is close to unity and does not vary much as the temperature is decreased, but below $T^*/N = 0.12$ it decreases fast, as the temperature is lowered, to 0.1 at $T^*/N = 0.04$.

Now we turn out attention to Fig. 3a, where we show the layer spacing as a function of the reduced temperature. We can clearly see that the lamellar width increases as the temperature is decreased. This is in agreement with theoretical calculations [10-14] which suggests the following scaling behavior:

$$D \propto T^{*\mu},\tag{8}$$

where $\mu = -1/6 \cong -0.17$. Fitting the data from Fig. 3a to the above function gives $\mu = -0.21$. This is close to $\mu = -1/6$ if we take into account that the theory was developed for strongly segregated microphases. The Self-Consistent Field Theory (SCFT) calculations by Banaszak and Whitmore [15] predict $\mu = -0.20$, in agreement with presented results.
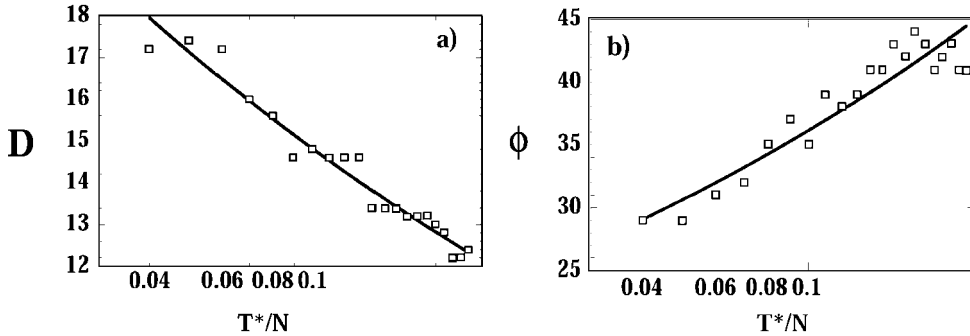
Fig. 3. Simulation results for 7-16-7 microarchitecture (solid line is a power fit): (a) lamellar periodicity as a function of T^*/N, below T_{ODT}; (b) bridging fraction as a function of T^*/N, below T_{ODT}

The triblock chains can form loops and bridges as defined in the Introduction. We can calculate the loops-to-bridges ratio, Φ, from the distribution of the triblock end-to-end distances in the direction normal to layers, defined as $r = \vec{R} \cdot \vec{n}$ where $\vec{n}$ is the normalized vector perpendicular to layers. We have looped configurations when $r \leq D/2$, whereas the larger distances correspond to the bridged configurations. In Figure 3b we report the bridging fraction, Φ. It decreases with decreasing temperature, as expected from theoretical calculations [11-13] suggesting the following scaling behavior:

$$\Phi \propto T^{*\tau},\tag{9}$$

where $\tau = 1/9 \cong 0.11$. Fitting the data from Fig. 3b to the above function gives $\tau = 0.24$. It is different from $\tau = 1/9$, but the above theories were developed for strongly segregated phases, and we fit the data up to the ODT temperature.
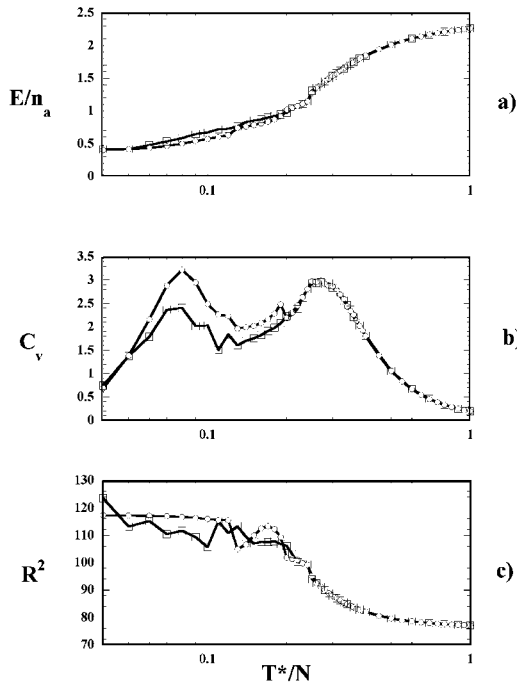
Fig. 4. Slow heating simulation results for the 7-16-7 microarchitecture (circles), and the corresponding quenching results (squares): (a) energy per lattice site, E^*/n_a; (b) specific heat, C_v; (c) squared end-to-end distance, R^2
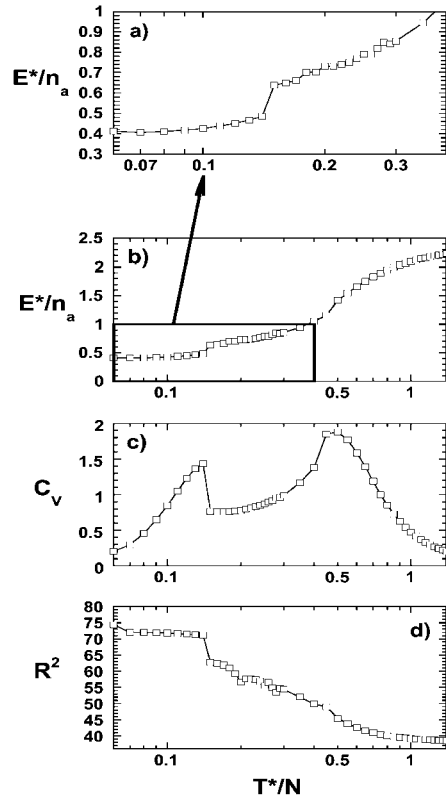
Fig. 5. Simulation results for the 8-8 diblock copolymer melt: (a) energy per lattice site, E^*/n_a, between the temperatures $T^*/N = 0.06$ and $T^*/N = 0.4$; (b) energy per lattice site, E^*/n_a; (c) specific heat, C_v; (d) squared end-to-end distance, R^2

In Figure 4 we present the data obtained from the slow heating experiments in comparison with the data obtained in quenching (Fig. 1). The slow-heating experiment is started from the configurations obtained from the $T^*/N = 0.04$ quenches. From this temperature the system is heated up in small temperature increments, $\Delta T^*/N = 0.01$. We can see that there is no major difference between data from quenching and heating experiments. There is only a small difference in energy below T_{ODT}, a higher low-temperature C_V peak in slow heating, and also significantly smoother R^2 in heating. However, smoother R^2 in the slow heating experiment is most likely caused by the lamellar spacing and orientation locking, that is trappings in metastable states.

Performing simulations for diblocks, similarly for triblocks, we can notice the low-temperature interfacial ordering. In Figs. 5a and 5b we report interaction energy per lattice size, E^*/n_a, as a function of the reduced temperature. The specific heat, calculated from Eq. 4, is shown in Fig. 5c. Figure 5d shows the mean squared end-to-end distance, R^2. The energy per lattice site decreases as the temperature is lowered. Close to the temperature $T^*/N = 0.5$ we report the fastest change of the energy. The squared end-to-end distance at high temperatures is close to the ideal Gaussian value, $(N - 1)a^2 = 30$, and it increases as the temperature is lowered. Close to the above mentioned temperature, where the specific heat peak is noticeable, the squared end-to-end distance also changes significantly. Taking into account all above considerations, we identify the temperature $T^*/N = 0.5$ as the order-disorder temperature, T_{ODT}, similarly as for triblocks. It is worth noting that this value ($T^* = 8.0$) is close to that obtained for the 7-16-7 triblocks ($T^* = 8.4$). Moreover, as we go towards lower temperatures, close to the $T^*/N \approx 0.15$, we can see the second peak in specific heat, another abrupt decrease of the energy, and a substantial stretching of the copolymer chains. This temperature roughly corresponds to the value T^*/N 0.08 recorded for the triblocks.

For triblocks we concluded that this low-temperature behavior is related to the interfacial ordering from the conventional lamellar phase to a lamellar phase with junction points sharply localized around a two-dimensional plane. The 8-8 diblock junction points are localized between 8th and 9th segment. Similarly as for the triblocks, we also calculate the Λ parameter shown in Fig. 6a. Comparing this with the data for the triblocks (Fig. 2) one can see that there are no significant differences in nature of the interfacial ordering. Finally, we notice that, since the 8-8 chains are shorter than the 7-16-7 ones, the interfaces between the diblock domains are less sharp at the corresponding low temperatures.

In Figure 6b we report the layer thickness, D. The layer spacing is obtained from the periodicity of corresponding concentration profiles in the direction of vector $\vec{n}$, the same way as presented above for the triblocks (Eq. 7). We can clearly see, that the layer thickness increases as the temperature is decreased with fastest change close to T^*/N 0.15. and below that temperature it remains almost unchanged. Applying the scaling relation (Eq. 8) suggested by the theoretical calculations [10-14] to fit the data from Fig. 6b gives $\mu = -0.25$. This result is close to that presented above for the triblocks ($\mu = -0.21$), and in fact it is close to theoretical predictions, $\mu = -1/6$, if we take into account both that the chains are very short and that the theory was developed for strongly segregated phases. We have to point out again, that it also very close to the SCFT predictions by Banaszak and Whitmore [15] who found $\mu = -0.20$ for diblocks.

Similarly as in the triblock analysis, Fig. 7 presents the data from heating experiment. We used the same technique as for the triblocks. The results obtained from heating experiment are in a qualitative experiment with the results from Fig. 5. In particular, we report two C_V peaks (Fig. 7c, the first one at $T^*/N = 0.5$ and the second one close to $T^*/N = 0.15$. Also the energy per lattice site, T^*/n_a, increases as the temperature is increased and the fastest change is similarly close to $T^*/N = 0.5$ (Fig. 7a and Fig. 7b). The squared end-to-end distance, R^2, as a function of the reduced temperature (Fig. 7d). decreases as the temperature is increased in agreement with data from Fig. 5d).
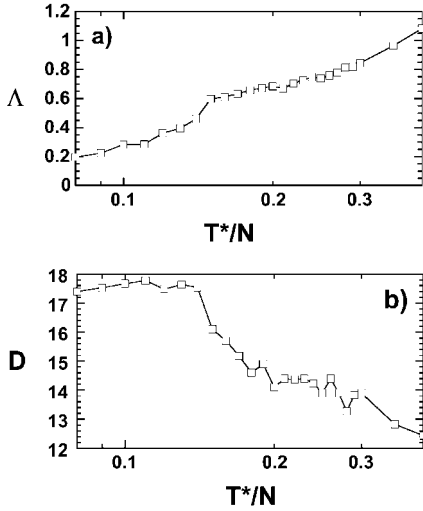
Fig. 6 (up). Results for the 8-8 co-polymer: (a) interfacial parameter, Λ as a function of T^*/N; (a) lamellar periodicity as a function of T^*/N
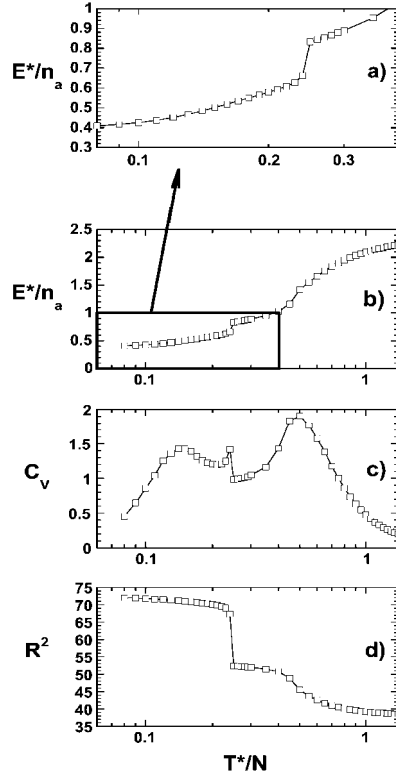
Fig. 7 (right). Slow heating simulation results for the 8-8 microarchitecture: (a) energy per lattice site, E^*/n_a; (b) specific heat, C_V; (c) squared end-to-end distance, R^2

Finally, we report the mean squared rotation angle after 10^6 MC steps, Θ^2, which can be considered proportional to the rotational diffusion constant, for the 8-8 diblock copolymer melt. In Fig. 8 we show Θ^2 the a function of the reduced temperature. The mean squared rotation angles, presented in Fig. 8, are decomposed into three Cartesian directions, where the direction X is parallel to the vector $\vec{n}$ (Eq. 7). The directions Y and Z, on the other hand, are parallel to the layers. Above the T_{ODT} there is no difference between rotational diffusions in three different directions, but below the order-disorder transition temperature we can notice a decoupling of the directional rotational diffusions into two branches. While the rotation diffusion in the X direction (normal to layers) does not change much as we decrease the temperature in the vicinity of the ODT, the rotational diffusion in Y and Z directions decreases abruptly below the ODT. Close to the temperature $T^*/N = 0.13$, in the vicinity of the low-temperature C_V peak, the rotational diffusion in directions parallel to layers (Y and Z) decreases abruptly once again.

Summarizing, we have to stress that the low-temperature C_V peak and the other low-temperature effects presented above occur both for the diblocks (T^*/N 0.15. $N = 16$) and for the triblocks ($T^*/N = 0.08$, $N = 30$) at roughly the same temperature ($T \approx 2.5$). The system with the thermal energy lower than the interaction energy is prone to sample only selective energy minima separated saddle points (Ref. [16] and therein). It is possible, therefore, that
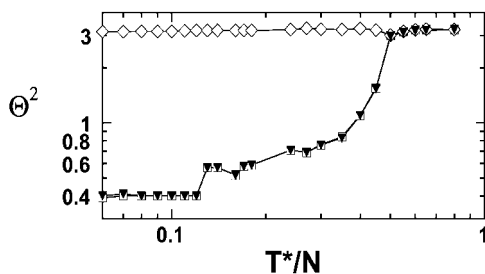
Fig. 8. Rotational diffusion, Θ^2, for the 8-8 diblock melt as a function of temperature, T^*/N, decomposed into X (open diamonds), Y (solid triangles), and Z (open squares) Cartesian directions; the direction X is normal to layers

low-temperature C_V peak is somehow associated with being trapped in the selective energy minima, and due to insufficient thermal energy not being able to sample the other energy basins. It is a kind of ergodicity breaking, but limited to the interfacial area because the parts of the blocks within the microdomains are free to move as in the athermal state $(\varepsilon_{AA} = \varepsilon_{BB} = 0)$.

4. CONCLUSION

The presented lattice-simulation data provide an additional evidence for the low-temperature ordering conjecture for block copolymer melts. These effects might be associated with sampling only the selective energy minima as suggested within the energy landscape framework. The reported phenomena reveal their signatures in both the static and the dynamic properties. However, there is still an urgent need to perform an off-lattice simulation to verify, whether the low-temperature interfacial ordering is based upon the existence of the underlying lattice or whether it is a property of the system regardless of the lattice.

References

[1] G. H. Fredrickson, V. Ganesan, and F. Drolet, Macromolecules **35**, 2002 (2002).
[2] M. W. Matsen and R. B. Thomson, J. Chem. Phys. **111**, 7139 (1999).
[3] S.-M. Mai, W. Mingvanish, S. C. Turner, C. Chaibundit, J. P. A. Fairclough, F. Heatley, M. W. Matsen, A. J. Ryan, and C. Booth, Macromolecules **33**, 03104 (2002).
[4] K. Karatassos, S. H. Anastasiadis, T. Pakuła, and H. Watanabe, Macromolecules 33, 523 (2000).
[5] M. Banaszak, S. Wołoszczuk, T. Pakuła, and S. Jurga, Phys. Rev. E **66**, 031804 (2002).
[6] M. Banaszak, S. Wołoszczuk, S. Jurga, and T. Pakuła, J. Chem. Phys. **119**, 11451 (2003).
[7] S. Woloszczuk, M. Banaszak, S. Jurga, T. Pakula, and M. Radosz, J. Chem. Phys. **1211**, 12044 (2004).
[8] T. Pakula, *Simulation Methods for Polymers,* ed. M. J. Kotelvanskv, D. N. Thedorou (Marcel-Dekker, 2004), chap. 5.
[9] L. Leibler, Macromolecules **13**, 1602 (1980).
[10] M. W. Matsen and M. Schick, Macromolecules **27**, 187 (1980).
[11] J. Huh, W. H. Jo, and G. ten Brinke, Macromolecules 35, 2413 (2002).
[12] E. B. Zhulina and A. Halperin, Macromolecules **25**, 5730 (1992).
[13] R. L. Jones, L. Kane, and R. J. Spontak, Chem. Eng. Sci. 51, 1365 (1996).
[14] A. Halperin and E. B. Zhulina, Europhys. Lett. 16, 337 (1991).
[15] M. Banaszak and M. D. Whitmore, Macromolecles **25**, 3406 (1992).
[16] P. G. Debenedetti and F. H. Stillinger, Naure 410, 259 (2001).